Compositional changes by SIMS and XPS analyses on fresh and aged Roman-like glass

AUTHORS
Roberta Zanini[a,b*], Giulia Franceschin[a], Elti Cattaruzza[b], Mirko Prato[c], Mario Barozzi[d], Arianna Traviglia[a*]
AFFILIATION
[a] Center for Cultural Heritage Technology, Istituto Italiano di Tecnologia, via Torino 155, Venice, Italy
[b] Dipartimento di Scienze Molecolari e Nanosistemi, Università Ca' Foscari Venezia, via Torino 155, Venice, Italy
[c] Materials Characterization Facility, Istituto Italiano di Tecnologia, Via Morego 30, 16163, Genoa, Italy
[d] Fondazione Bruno Kessler, via Sommarive 18, 38123, Trento, Italy

ABSTRACT:

This study reports important analytical evidence of an unusual non-uniform element distribution in the superficial layers of glass matrices (from few nm up to 1 micron). The unforeseen observation was made on silica-soda-lime glass mock-ups before and after their artificial ageing, using secondary ion mass spectrometry (SIMS) and X-ray photoelectron spectroscopy (XPS) surface analysis techniques. The analyses showed a marked non-homogeneous element distribution at the glass surface. The results indicated a very low concentration of Na at the surface up to a depth of around 500 nm below the surface, where its concentration increases reaching a plateau. In addition, the profile distribution of H in the first 200 nm of the pristine glass surface indicated a diffusion of hydrogen from the surrounding environment to the glass network. Additional modifications during the glass ageing process related to external factors (such as temperature and humidity) were also identified in relation to sodium atoms, with atoms on the glass surface showing a different chemical state from those in the bulk. This study confirms that glass composition as well as glass alteration are non-homogeneous locally supporting the importance of studying glass surface as region of interaction with surrounding environment.

Keywords: Glass corrosion, glass surface, surface analysis, XPS, SIMS.

Highlights

The combined use of SIMS and XPS enables to examine composition of glass surfaces.

XPS and SIMS analyses show composition gradient of fresh soda-lime glass surfaces.

Artificial ageing induces chemical and compositional modification of glass surfaces.

An articulated analysis approach is used to shed light on glass corrosion.

1. Introduction.

Glass has unique properties. In standard conditions, the combined characteristics of transparency and hardness, coupled with good mechanic strength and excellent corrosion resistance, make the use of glass highly suitable for many applications and situations, spanning from the manufacture of artistic objects (e.g., stained glass) to the fabrication of industrial and technological products (e.g., windows on a spacecraft). Glass, however, is subject to corrosion and clear evidence of the transformation of its vitreous structure when subjected to the action of aggressive agents – such as humidity, water, strong acidic/alkaline solutions [1] - can be easily observed on everyday objects. Unsurprisingly, an analogous phenomenon can also be detected – in a magnified form – on ancient glass, as seen in archaeological items produced with this material. Advances in research on chemical corrosion of glass is therefore equally important for both the preservation and protection of modern glass and for the conservation of historical and archaeological glass objects, which have undergone similar stresses for a (much) longer period.

The mechanism of glass alteration depends both on the nature of the glassy material – i.e., its chemical composition and structure– and on external factors such as, for example, the amount of water that reacts with the glass object surface in presence of humidity, the pH of a solution interacting with it, and the time of the reaction [2]. Due to the many and different factors involved, the glass corrosion process is still not entirely understood and different theories have been formulated to explain it.

Among them, two are the most reliable [3]: the Classic Inter-Diffusion (CID) model, and the more recent Interfacial Dissolution-Reprecipitation (IDP) model. The first considers the diffusion-controlled hydrolysis and ion exchange reactions as the main processes that support the preferential dissolution of more soluble cations during the initial part of the leaching process. The second instead, is based on the congruent dissolution of silicate glass coupled with the reprecipitation of amorphous silica aggregates: dissolution and reprecipitation support the glass corrosion without interdiffusion-controlled ion-exchange mechanisms at the glass reaction front.

The goal of this study is to propose a different and refined approach for characterising glass surface, namely region where the initial processes of glass alteration take place. This paper reports on the chemical configuration of glass surface samples as pristine objects, after annealing treatment, and after artificial ageing.

Standard procedures to experimentally study the ageing effects on glass consist of preparing artificial glass replicas and investigate the various artificial wearing-out stages, by using analytic techniques able to provide compositional and chemical information about the glass surface [4]. X-ray fluorescence (XRF) spectroscopy [5], optical microscopy, scanning

electron microscopy (SEM) [6] and Raman or Infrared spectroscopy [7] are normally used to investigate the chemical composition of altered glass, its surface morphology, and the corrosion products present on it.

X-ray Photoemission Spectroscopy (XPS) [8–13] and Secondary Ion Mass Spectrometry (SIMS) [14-17] are sometimes used too, even if their contemporary use to investigate the corrosion mechanism of glass is quite limited. We show here that their combined use can be effectively useful for a better characterisation of corroded glass surfaces: with this approach we were able to evidence important element distribution gradient on the superficial layers of our glass matrices, ranging from the first few nm of the surface to a depth around 1 micron, as well as a lateral non-uniform element distribution on the scale of few tens of microns.

2. Material and Methods.

The investigated matrices were silica-soda-lime (SSL) glass prepared by *Stazione Sperimentale del Vetro (SSV) – The glass research centre*, a specialized laboratory based in Murano (Venice, Italy). Replica samples were realized following the typical composition of Roman SSL glass type, with a high content of SiO_2, CaO, and Na_2O, and low concentration of MgO and K_2O. The presence of impure raw materials (to replicate the inclusion of various minerals contained in ancient sand) was achieved by adding in the glass mock-ups heavy metals, such as Fe and Cu. Mn and Sb oxides were added as bleaching agents. Table 1 reports the chemical composition of the glass replicas, as obtained by Wavelength Dispersive X-ray Fluorescence (WD-XRF).

For the samples preparation, the raw materials were heated at 1400°C in a platinum crucible to reach the melting point and the resulting molten glass was slowly cooled until complete solidification. The raw materials used and their quantities are listed in Table 2. The raw glass was annealed at 550°C for 1 hour and then slowly cooled down to room temperature for 1 day to prevent the formation of mechanical stress, due to gradients of temperature between surface and bulk of the glass object. The melt was homogenised a few times during the fusion using a platinum stick. The raw glass was then thinly sliced (10×10×2 mm^3) to create the testing samples.

Table 1. Chemical nominal composition of SSL glass mock-up (in wt% oxide and at%).

Oxide	wt%	Element	at%
SiO_2	67.6	Si	23.49
Al_2O_3	1.97	Al	0.81
Na_2O	18.6	Na	12.53
K_2O	0.40	K	0.18
MgO	0.68	Mg	0.35
CaO	8.05	Ca	2.99
SO_3	0.24	S	0.06
Sb_2O_3	0.10	Sb	0.01
P_2O_5	0.14	P	0.02
Fe_2O_3	0.68	Fe	0.18
MnO	0.59	Mn	0.17
CuO	0.10	Cu	0.03
CoO	<0.01	Co	0.00
Cl	0.9	Cl	0.53
TiO_2	0.02	Ti	0.005
		O	58.65

Table 2 Raw materials used for the mock-up's preparation.

Raw material	(grams)
Siliceous sand	560.77
Sodium carbonate	247.74
Calcium carbonate	104.75
Dolomite	22.88
Hydrated alumina	25.35
Manganese dioxide	6.11
Calcium diphosphate	2.24
Iron oxide	5.78
Potassium carbonate	6.06
Antimony oxide	0.84
Sodium chloride	13.68
Copper oxide (dark)	0.84
Sodium sulphate	2.96
Tot	**1000.00**

The SIMS depth profiles were obtained with a dynamic SIMS SC-ultra, with Cs^+ primary ion sputtering beam at 3 keV of impact energy and 64° incidence angle. The acquired secondary species are positive MCs^+ molecular ions, where M indicates each elements of interest. All SIMS data were normalised point by point to the Cs^+ secondary ion signal acquired at the same depth. This normalisation method takes into account the possible drifts on the secondary ion intensities induced by charging effects when the ion beam erodes dielectric samples as glass. A thin gold capping layer was deposited on all sample surfaces: this conductive layer and the use of an electron flood gun are needed to remove the excess of positive electric charge induced by the Cs^+ ion sputtering. All depth profiles have been normalised to the average silicon intensity in the glass bulk. The relative intensities - in counts per second - among the different secondary ion species do not represent the true relative concentrations, being related on strongly different ion yields. The depth scale was calibrated with the measurement of the final sputtered crater depth, by using a Tencor P6 mechanical profilometer and supposing a constant erosion speed.

X-ray Photoelectron Spectroscopy (XPS) analyses were carried out with a Kratos Axis Ultra^{DLD} spectrometer using a monochromatic Al Kα source (20 mA, 15 kV). Survey scan analyses were carried out with an analysis area of 300 x 700 microns and a pass energy of 160 eV. High resolution analyses were carried out with the same analysis area and a pass energy of 20 eV. The Kratos charge neutraliser system was used on all specimens. Charge compensation and calibration of the binding energy (BE) scale were done by setting the BE of Si2p band at 103.4 eV [18–20]. The use of an internal reference (Si2p) was preferred to the usual C1s position for the adventitious (hydro)carbon contamination layer because in literature the C-C/C-H signal is reported to fall in a very large BE range (284.0–285.6 eV), thus making a reliable energy scale calibration extremely difficult [21,22]. The use of Si2p reference gave for the C1s adventitious hydrocarbon a BE around 285.5 eV in all the analysed samples, which is in line with the values reported in literature [21,22]. Deconvolution of the different components in the XPS signals were performed with XPSPEAK41 software [23]. The final uncertainty on the determined BE is around 0.2 eV.

2.1. Experimental

For both SIMS and XPS analysis, the glass surface was not polished to maintain the original chemical information of the top layers: all the samples were simply washed following an internal protocol, using soapy water, deionized water, acetone, trichloroethylene, and absolute ethanol with 5 minutes of sonication for each immersion in any single solvent. Analyses were performed on a “virgin surface”, i.e., not on the sliced ones.

SIMS analysis of the glass sample was repeated in 4-5 different points of the sample surface and performed both before (pristine glass) and after an annealing treatment at 600 °C for 6 hours in air. The in-depth analysis was performed until element concentration reached a plateau (bulk values).

XPS analysis of the glass samples was performed immediately after the reported mild cleaning treatment on pristine glass both on the sample surface (sample named “T0”) and on the inner region immediately after fracturing the sample (sample named “T0 bulk”). The XPS analysis of the glass surface was carried out also after two weeks of artificial ageing of the sample in a climatic chamber with constant temperature of 80°C (sample named “T1”). The relative humidity level RH was kept at 90% for the first week, then it was lowered down to 30% for the second week. Only pure water (MilliQ) was used during the artificial ageing, thus preventing any undesired effect of interaction between the samples and the external agents (e.g., salts present in tap water). XPS quantitative results are reported before and after the correction for hydrocarbon contamination layer [24]; its presence causes the attenuation of photoelectron signals coming from elements present just below the contamination layer, thus masking the true atomic concentrations. Therefore, reported quantitative data are characterized by relative random uncertainties around 10% but systematic errors can be larger due to the complexity of the systems under investigation. For preserving the original surface, we decided to avoid ion sputtering, thus preventing preferential sputtering and/or induced chemical changes of the surface atoms.

3. Results and Discussion.

The results of the SIMS analysis are reported in Fig. 1 for two different point of the pristine sample, showing the concentration profile of the monitored elements from the first layers of the surface up to 1-2 microns inside. The different concentration of alkaline ions (Na^+) between the surface and the deeper region of the samples is evident. The elemental profiles show a sharp increase of Na concentration at about 350-400 nm from the surface, after which it stabilises on a quite constant (bulk) value. Differently, silicon and aluminium (glass formers), and calcium (alkaline-earth stabiliser) were detected with homogeneous concentration from the surface to the bulk of the sample.

The Na depletion in the first 350-400 nm under the surface can be possibly explained with the loss of volatile Na from the surface of melt glass during its preparation process. Evaporation of glass melt components commonly leads to the depletion of volatile glass compounds at the surface layer of a melt [25], a phenomenon remediated by annealing the solidified glass at proper temperatures. However, the time and temperature adopted for the

annealing treatments may be sometimes insufficient to assure a complete homogenisation in the composition.

The compositional analysis of the pristine glass revealed the presence of hydrogen ions in the first 200 nm of the glass surface (Fig. 1). This can be due to the diffusion of water molecules into the glass network when the freshly made glass encounters surrounding air (during glass cooling), which results in the formation of a water film on the surface of glass. The possibility that the presence of hydrogen could be originated by molecular hydrogen diffusion should also be considered.

The SIMS profiles obtained analysing the pristine glass (T0) clearly indicated the presence of a region under the glass surface marked by very low concentration of sodium, which rises at a depth of about 0.5 μm. A similar trend has been observed in different points of the samples. Then, we repeated SIMS measurements after an annealing treatment at 600°C, to check the Na mobility into the glass network, and to verify if it would be redistributed into the depleted region. Data collected on different points of the sample surface (Fig. 2) indicated an extreme variability of the heat treatment effect, showing in some cases a redistribution of Na to reoccupy the superficial layer initially depleted of Na (Fig. 2 point 2 and 3), while in some others (point 1) a progression of the alkaline emptying zone, interesting more than one micron into the glass bulk. Considering more closely the shape of the signal related to sodium, in point 2 and 3 of Fig. 2 the slope variations in the region around 500 nm is consistent with a back-diffusion (i.e., toward the surface) of sodium induced by the thermal treatment.

The sodium atoms concentration was high only at depths larger than 400 nm before the thermal treatment. In point 1 of Fig. 2, instead, the sodium depth profile does not show a similar behaviour: even if this profile could suggest an increase of the depletion zone induced by the thermal treatment, we cannot exclude that here the starting depletion was much larger than 400 nm. This lacking compositional homogeneity in the first microns below the glass surface is not only detected by varying the depth but also laterally at the same depth: Fig. 3 shows the Na distribution map (in direct image) at the start and at the end of the in-depth profile, showing a marked non-uniform lateral presence of Na in the whole analysed glass region, as additional evidence of inhomogeneity of the local glass composition.

All these experimental findings showed that the composition of the first 1-2 microns of the glasses under analysis (before and after the additional thermal treatment) is far from being homogeneous. Moreover, the evidence of an extended surface region with a sodium depletion on the pristine glass should force us to think different about the glass degradation mechanisms usually considered, being them strongly dependent on the starting composition of the glass surface [26].

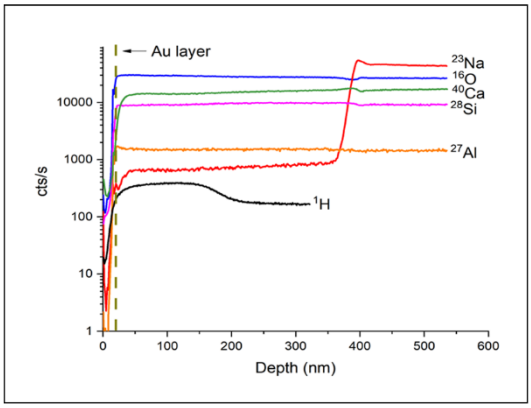

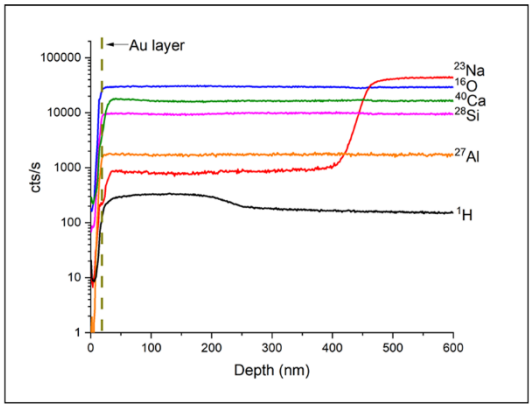

Figure 1. The element depth profile of pristine silica-soda-lime in two different point of mock-up.

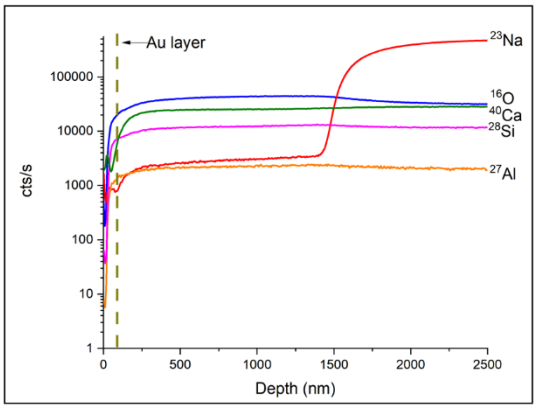

Point 1

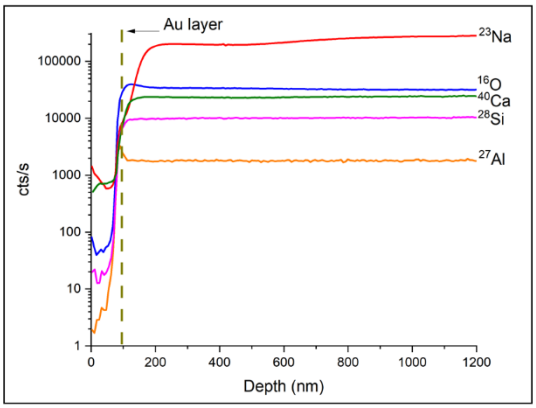

Point 2

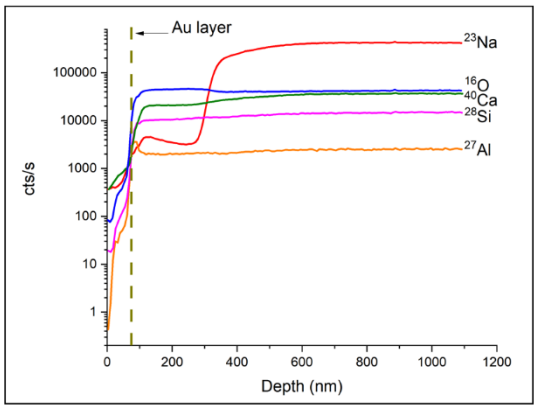

Point 3

Figure 2. The element depth profile on three different point of silica-soda-lime mock-up after annealing treatment at 600°C for 6 hours.

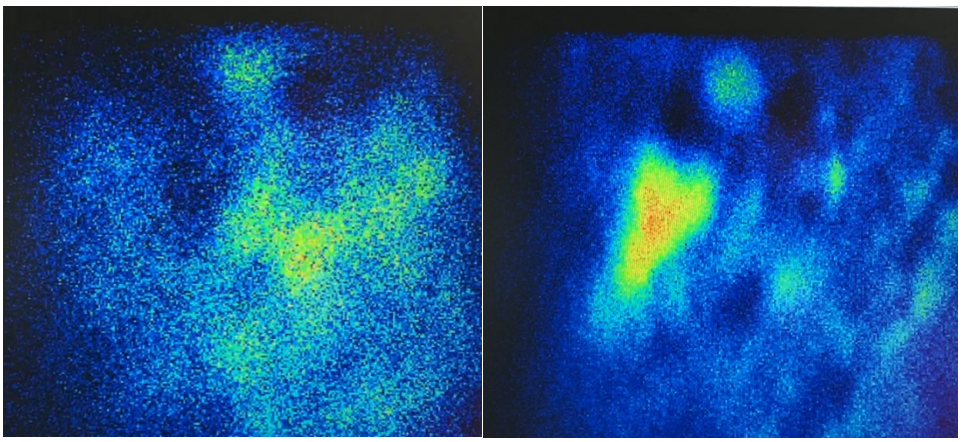

Figure 3. SIMS maps with the planar distribution of the intensity of ^{23}Na ion signal at the start (left panel) and at the end (right panel) of the SIMS analysis after sample annealing. The analysed area is 300×300μm^2. Intensity increases from blue to jellow to red.

XPS provided complementary information thanks to its extremely superficial sampling depth (5-10 nm), thus enabling investigation of the top layers of the glass surface. Table 3 (first column) reports the average values of surface composition of the sample before (T0 pristine and T0 bulk) and after (T1) the two weeks of artificial ageing, in which a large amount of carbon contamination is present (C1s signal centred around 285.5 eV of BE). Considering the experimental errors and after the correction for the carbon contamination, as explained below, the elements concentration of the glass bulk obtained by XPS analysis (sample named "T0 bulk") is in very good agreement with the nominal composition of glass mocks-ups measured using WD-XRF (at % in Table 1).

From the analytical point of view, it is incorrect to perform a quantitative data renormalisation simply excluding the carbon contribution (Table 3, second column): the presence of the hydrocarbon contamination layer on the top of the surface induces the attenuation of the photoelectron signals coming from the other elements in the sample, but this intensity reduction is different for different elements because it depends on the photoelectron kinetic energy. We consider as covering contamination layer only the amount of carbon forming hydrocarbon contamination and detected as the low BE component of C1s band (around 80% of the whole C1s intensity, after deconvolution procedure [23]), thus assuming that the other carbon atoms are involved in chemical bonds with the glass matrix surface.

Based on the work of G.C. Smith [24] we were then able to give a rough estimation of the contamination layer thickness (0.6 nm for T0; 0.6 nm for T0 bulk; 4.9 nm for T1) and the consequent correction of calculated composition (Table 3, columns named "after correction"). We are well aware that the determination of the contamination layer thickness (thus, of the final composition) assumes that all the detected (hydro)carbon contamination originates from a homogeneous and constant-in-thickness contamination layer, covering the whole sample surface. If we reasonably assume that some region of the sample surface could be differently covered (or maybe uncovered) by carbon contamination, then the true values of the relative atomic composition of the investigated surface should lie in the range determined by the values reported in 2nd and 3rd column of Table 3.

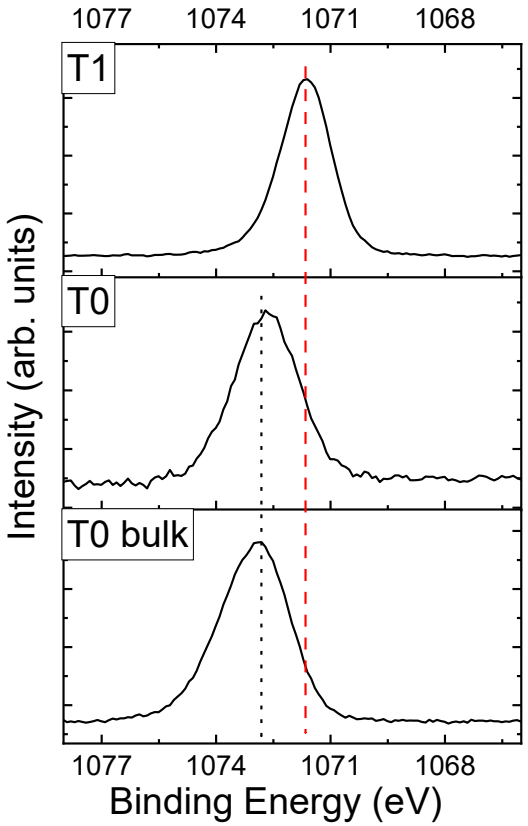

Figure 4. Na1s band recorded on the three samples.

The concentration of sodium in the pristine glass at time T0 is much lower on the surface than in the bulk of the sample (T0 bulk), and the Na1s band is centred around 1072.7 eV and 1073.0 eV of BE, respectively. On the other hand, after two weeks of artificial ageing, sodium concentration on the superficial layers of the sample increases abruptly (Table 3), while the concentrations of calcium and, in particular, of silicon decrease. The Na concentration ~~is~~ increment is a clear evidence of chemical driving forces inducing diffusion and accumulation of sodium atoms on the first few nm of surface layers when glass is subjected to unfavourable environmental conditions (high temperature and humidity). This superficial accumulation determines the presence of a zone of aggregation and disorder in which the compositional and structural properties are different from those determining the macroscopic physico-chemical behaviour of glass, as testified by the different BE detected for the Na1s band at time T1 (1071.7 eV).

In summary, the Na1s peak of the analysis at T0 has a similar BE both for surface and bulk analysis, but at time T1 the BE of Na1s shifts at lower value (Fig. 4). This change of BE may be indicative of a different nature of sodium: in the pristine glass, sodium acts as modifier ion in the glass network; conversely, after an artificial alteration (sample at T1) the sodium detected by XPS is present in a different chemical environment, most likely as sodium carbonates [18,27] formed on the glass surface. The chemical stress induced on the glass mock-up by artificial ageing – characterised by high level of temperature and humidity - caused

the leaching of sodium and its accumulation on the surface, where it can react with the surrounding environment.

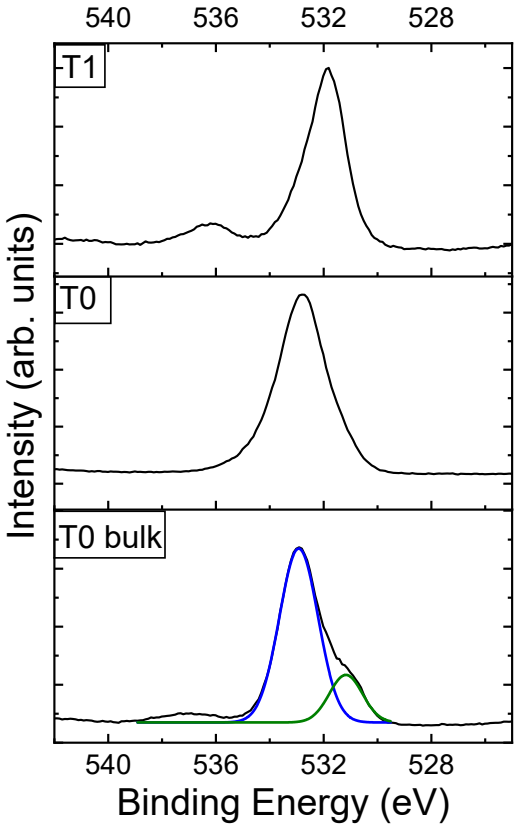

Figure 5. O1s band recorded on the three samples. The small signal around 537 eV is originated by Na Auger electrons.

The formation of sodium oxides/carbonates on T1 sample was suggested also by the analysis of the O1s band (Fig. 5). The signal centred around 536-537 eV is not related to oxygen, being part of the NaKLL band: its different relative intensity in the three samples is directly related to the different Na amount, as reported in Table 3. About the true O1s signal, in the T0 bulk sample the band clearly showed the presence of two components (bottom panel of Fig. 5), falling around 532.9 eV and 531.2 eV and related to BOs (Bridging Oxygens) and to NBOs (Non-Bridging Oxygens), respectively: these signals are characteristics of soda-lime silicate glasses [10]. On the surface of the pristine glass (T0 sample), the lower amount of Na induces a decrease of the NBOs band intensity. In the T1 sample, the different composition of the surface – rich in sodium and strongly contaminated by carbon – affects the structure of O1s band. Indeed, the BOs band is reduced in intensity, and a new more intense component appears, centred on 531.9 eV of BE. This band can be attributed to the presence of Na carbonates at the sample surface [18,27], formed during the ageing process.

Analysis of C1s signal recorded on T1 sample confirmed the possible presence of carbonates (Fig. 6) because, in addition to the main component related to adventitious carbon contamination usually falling in a wide range of BE (roughly between 284-286 eV [21,22]; in our

three samples around 285.5 eV), a less intense band centred at 289.0 eV is detected. This last band is consistent with the presence of sodium carbonates [18,27], and/or of sodium hydrocarbonates.

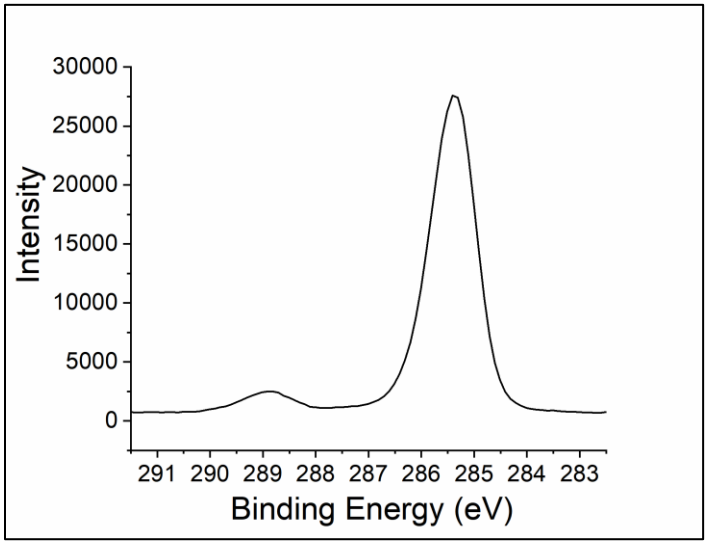

Figure 6. C1s band recorded on the T1 sample.

It is well-known that humid air and water are the first cause of degradation of glass, inducing a decrease in alkali ion concentration and increasing the local pH value (see, for instance, [12,28,29]).Considering the XPS experimental findings in this work, we suggest the following possible corrosion mechanism starting at the glass surface and involving water and CO_2 from the atmosphere, in addition to $H^+ \leftrightarrow Na^+$ ion exchange at the first few nm of the sample surface [30,31]:

[1] $CO_2 + H_2O \rightarrow H^+ + HCO_3^-$

[2] $HCO_3^- + Na^+ \rightarrow NaHCO_3$

The formation of these kinds of compounds can lead to a pH increase on the glass surface towards more alkaline value, that should favour further glass corrosion. However, this hypothesis will need further investigation, for instance by analysis of samples aged for longer periods.

The presence of the Na2s band is easily visible in the low BE region of the XPS survey (not reported). This signal is originated by photoelectrons having high kinetic energy, thus coming also from Na atoms that are present in deeper regions of the sample surface [10]. With the used instrument, the expected intensity ratio of Na1s and Na2s bands (Na1s/Na2s) is around 10 for a homogeneous sample, based on the so-called RSF (Relative Sensitivity Factor) [10]. The different intensity ratio experimentally detected on the three samples for these two Na signals, Na1s/Na2s (Table 3), showed a very low value for the T0 sample, suggesting that an

important sodium concentration gradient is present also in the first 5-10 nm of the surface, with a marked depletion in the first few layers (possibly 1-2 nm) of the region investigated by the XPS technique. For T0 bulk and T1 the Na1s/Na2s value is higher, suggesting a more homogeneous distribution of the element.

The photoelectron intensity attenuation effect induced by the contamination layer does not change the previous conclusion, since the contamination thickness ~~is the same~~ for T0 and T0 bulk samples is quite the same.

Table 3. Average composition data obtained by XPS analyses on the surface of the pristine glass (T0), on the bulk of the pristine glass (T0 bulk), and on the surface after two weeks of artificial ageing (T1). All the reported data are expressed in atomic percentage (see text for explanation). We consider as covering contamination layer only the amount of carbon related to hydrocarbon contamination, i.e. not including other carbon atoms. The last column shows the detected intensity ratio of Na1s and Na2s bands. Relative uncertainties of the calculated concentrations are around 10% of the reported values.

	BEFORE CORRECTION (at %)			**BEFORE CORRECTION (without hydrocarbon) (at %)**			**AFTER CORRECTION (at %)**			**Na1s/Na2s**		
	T0	T0 bulk	T1	T0	T0 bulk	T1	T0	T0 bulk	T1	T0	T0 bulk	T1
Al 2p	2.3	0.5	-	2.7	0.6	-	2.6	0.5	-			
C 1s (contam.)	16.6	15.4	75.3	-	-	-	-	-	-			
C 1s (other)	2.6	2.7	5.7	3.4	3.2	23.1	2.8	2.9	6.7			
Ca 2p	2.4	2.3	0.6	2.9	2.7	2.4	2.8	2.6	1.2			
Cu 2p	0.2	-	0.1	0.2	-	0.4	0.3	-	0.8			
Mg 2p	0.1	0.3	0.1	0.1	0.3	0.4	0.1	0.3	0.1			
Na 1s	1.0	8.8	3.4	1.2	10.4	13.8	1.5	12.8	54.3	5.2	8.3	8.3
O 1s	52.0	47.4	12.6	62.3	56.1	51.0	63.8	55.9	33.4			
Si 2p	22.7	22.6	2.2	27.1	26.7	8.9	26.0	25.0	3.5			
Zn 2p	0.1	-	-	0.1	-	-	0.1	-	-			

The results obtained by XPS and SIMS analyses confirmed the different elemental composition of glass network in the bulk and in the first 1-2 microns of the surface. In particular, the in-depth elemental profiles showed the different mobility of glass formers and glass modifiers (in particular, Na) during both the melting and cooling processes of the glass preparation, as well as the interaction of the surface of the final glass with the surrounding environment [32]. It is likely that sodium atom concentration at the glass surface differs from the bulk material because of sodium volatility during the glass melt [33-35].

Descriptions of the detected behaviour and a similar marked in-depth and lateral concentration difference of alkaline elements were difficult to find in literature. Papers describing investigation of glass corrosion by SIMS technique reported approaches that did not deliver the

same experimental findings here described, probably because SIMS was usually not performed beyond 100-200 nm of depth from the surface. Actually, authors reported SIMS analysis of aged glass assuming they had the same composition along the entire sample (i.e., from the surface to the bulk), or polished the glass samples before the artificial alteration, thus losing crucial information about the first few hundreds of nm of the pristine glass [4,36–38].

The investigation of the glass surface performed in this work allowed to evidence an extended compositional transition region between the glass bulk and the environment in lieu of an abrupt hiatus. Marked lateral inhomogeneity of sodium distribution were highlighted too, on a scale of few tens of microns. All these experimental findings, obtained by performing both SIMS and XPS analyses on the glass surfaces, suggest that a comprehensive study of glass degradation mechanisms must take into account that this material may be highly inhomogeneous in the region of interaction with the surrounding atmosphere.

4. Conclusions

This study provides analytical evidence of the heterogeneity in the chemical composition of the surface of Roman-like glass and the surface modification – before and after the artificial ageing – related to the interaction with external factors (temperature and humidity). We evidenced important changes in the glass surface composition, mainly related to Na atoms both in the first few nm and on a scale of some hundreds on nm.

In the first few hundreds of nm the sodium content appears lower than the bulk value, probably because it vaporises in some regions of the glass surface due to its volatile nature under glass melting conditions. In addition, sodium appeared to be non-homogeneously distributed laterally too. The possibility of marked inhomogeneity of soda-lime glass composition in the first few hundreds of nm below the surface (mainly related to sodium content variations) must be considered also in the case of modern and industrial glasses obtained by manufacturing technologies, as well as for a better understanding of the ancient glass corrosion mechanism, with the final aim to develop new solution for its conservation. Work is in progress to study the evolution of the glass surface modification already evidenced: analysis of glass subjected to artificial ageing for longer times should allow to understand if the formation of sodium carbonates on the glass surface could be a first step towards the irreversible alteration of the matrix.

Acknowledgements

The authors would like to thank the Stazione Sperimentale del Vetro of Murano (Venice-Italy) for the preparation of glass mock-ups used in this work.

References

[1] N.A.R. van Giffen, S.P. Koob, Deterioration of Vitreous Materials, in Encycl. Archaeol. Sci. (2018). https://doi.org/10.1002/9781119188230.saseas0179

[2] G. Verhaar, Glass sickness: Detection and prevention Investigating unstable glass in museum collections, PhD thesis, UvA-DARE (Digital Academic Repository), (2018). https://hdl.handle.net/11245.1/669f19fd-9169-40f7-aec3-8bd568d9ab8c
[3] C. Lenting, O. Plümper, M. Kilburn, P. Guagliardo, M. Klinkenberg, T. Geisler, Towards a unifying mechanistic model for silicate glass corrosion, npj Mater. Degrad. 2 (2018) 28. https://doi.org/10.1038/s41529-018-0048-z
[4] A. Tournié, P. Ricciardi, P. Colomban, Glass corrosion mechanisms: A multiscale analysis, Solid State Ionics 179 (2008) 2142–2154. https://doi.org/10.1016/j.ssi.2008.07.019
[5] F. Gherardi, Compositional and Morphological Investigations of Roman Glass from Cremation Deposits at Birdoswald Fort on Hadrian's Wall, UK, Heritage 5 (2022) 362–377. https://doi.org/10.3390/heritage5010021
[6] O. Schalm, G. Nuyts, K. Janssens, Some critical observations about the degradation of glass: The formation of lamellae explained, J. Non-Cryst. Solids 569 (2021) 120984. https://doi.org/10.1016/j.jnoncrysol.2021.120984
[7] M.E. Lynch, D.C. Folz, D.E. Clark, Use of FTIR reflectance spectroscopy to monitor corrosion mechanisms on glass surfaces, J. Non-Cryst. Solids 353 (2007) 2667–2674. https://doi.org/10.1016/j.jnoncrysol.2007.05.012
[8] D. Sprenger, H. Bach, W. Meisel, P. Gütlich, XPS study of leached glass surfaces, J. Non-Cryst. Solids. 126 (1990) 111–129. https://doi.org/10.1016/0022-3093(90)91029-Q
[9] Y. Yamamoto, Precise XPS depth analysis of soda-lime-silica glass surface after various treatments, Surf. Interface Anal. 44 (2012) 931–933. https://doi.org/10.1002/sia.4836
[10] G. Pintori, E. Cattaruzza, XPS/ESCA on glass surfaces: A useful tool for ancient and modern materials, Opt. Mater. X. 13 (2022) 100108. https://doi.org/10.1016/j.omx.2021.100108
[11] B. Dal Bianco, R. Bertoncello, L. Milanese, S. Barison, Surface study of water influence on chemical corrosion of Roman glass, Surf. Eng. 21 (2005) 393–396. https://doi.org/10.1179/174329305X64376
[12] B. Dal Bianco, R. Bertoncello, L. Milanese, S. Barison, Glasses on the seabed: surface study of chemical corrosion in sunken Roman glasses, J. Non-Cryst. Solids 343 (2004) 91–100. https://doi.org/10.1016/j.jnoncrysol.2004.07.002
[13] B. Dal Bianco, R. Bertoncello, L. Milanese, S. Barison, Glass corrosion across the Alps: A surface study of chemical corrosion of glasses found in marine and ground environments, Archaeometry 47 (2005) 351–360. https://doi.org/10.1111/j.1475-4754.2005.00206.x
[14] A. Rodrigues, S. Fearn, M. Vilarigues, Historic K-rich silicate glass surface alteration: Behaviour of high-silica content matrices, Corros. Sci. 145 (2018) 249–261. https://doi.org/10.1016/j.corsci.2018.10.010
[15] S. Fearn, D.S. McPhail, B. Hagenhoff, E. Tallarek, TOF-SIMS analysis of corroding museum glass, Appl. Surf. Sci. 252 (2006) 7136–7139. https://doi.org/10.1016/j.apsusc.2006.02.157
[16] J.J. Neeway, S. Kerisit, S. Gin, Z. Wang, Z. Zhu, J.V. Ryan, Low-temperature lithium diffusion in simulated high-level boroaluminosilicate nuclear waste glasses, J. Non-Cryst. Solids 354 (2008) 4952–4958. https://doi.org/10.1016/j.jnoncrysol.2014.08.053

[17] M. Collin, S. Gin, P. Jollivet, L. Dupuy, V. Dauvois, L. Duffours, ToF-SIMS depth profiling of altered glass, npj Mater. Degrad. 3 (2019) 14. https://doi.org/10.1038/s41529-019-0076-3
[18] NIST X-ray Photoelectron Spectroscopy Database - NIST Standard Reference Database 20. https://doi.org/http://dx.doi.org/10.18434/T4T88K
[19] A. Vanleenhove, F.C. Mascarenhas, I. Hoflijk, I. Vaesen, C. Zborowski, T. Conard, HAXPES on SiO_2 with Ga Kα photons, Surf. Sci. Spectra 29 (2022) 014012. https://doi.org/10.1116/6.0001523
[20] S.M. Castanho, R. Moreno, J.L.G. Fierro, Influence of process conditions on the surface oxidation of silicon nitride green compacts, J. Mater. Sci. 32 (1997) 157–162. https://doi.org/10.1023/A:1018543703475
[21] G. Greczynski, L. Hultman, X-ray photoelectron spectroscopy: Towards reliable binding energy referencing, Prog. Mater. Sci. 107 (2020) 100591. https://doi.org/10.1016/j.pmatsci.2019.100591
[22] G. Greczynski, L. Hultman, The same chemical state of carbon gives rise to two peaks in X-ray photoelectron spectroscopy, Sci. Rep. 11 (2021) 11195. https://doi.org/10.1038/s41598-021-90780-9
[23] K. Raymund, XPS PEAK 4.1. free software
[24] G.C. Smith, Evaluation of a simple correction for the hydrocarbon contamination layer in quantitative surface analysis by XPS, J. Electron Spectrosc. Relat. Phenom. 148 (2005) 21–28. https://doi.org/10.1016/j.elspec.2005.02.004
[25] H. Van Limpt, R. Beerkens, O. Verheijen, Models and Experiments for Sodium Evaporation from Sodium-Containing Silicate Melts, J. Am. Ceram. Soc. 89 (2006) 3446–3455. https://doi.org/10.1111/J.1551-2916.2006.01233.X
[26] L.L. Hench, Characterization of glass corrosion and durability, J. Non-Cryst. Solids 19 (1975) 27–39. https://doi.org/10.1016/0022-3093(75)90067-8
[27] R. Würz, M. Rusu, Th. Schedel-Niedrig, M.Ch. Lux-Steiner, H. Bluhm, M. Hävecker, E. Kleimenov, A. Knop-Gericke, R. Schlögl, In-situ X-ray photoelectron spectroscopy study of the oxidation of $CuGaSe_2$, Surf. Sci. 580 (2005) 80–94. https://doi.org/10.1016/j.susc.2005.01.054
[28] R.H. Doremus, Interdiffusion of hydrogen and alkali ions in a glass surface, J. Non-Cryst. Solids 19 (1975) 137–144. https://doi.org/10.1016/0022-3093(75)90079-4
[29] M.M. Curtin Carter, N. Stewart McIntyre, H.W. King, A.R. Pratt, The aging of silicate glass surfaces in humid air, J. Non-Cryst. Solids 220 (1997) 127–138. https://doi.org/10.1016/S0022-3093(97)00301-3
[30] I. S. T. Tsong, C. A. Houser, W. B. White, A. L. Wintenberg, P. D. Miller, and C. D. Moak, Evidence for interdiffusion of hydronium and alkali ions in leached glasses, Applied Physics Letters 39, (1981) 669. doi: 10.1063/1.92814
[31] X Li, L. Jiang, J. Liu, M Wang, J Li, Y Yan, Insight into the Interaction between Water and Ion-Exchanged Aluminosilicate Glass by Nanoindentation, Materials (Basel) 30 (2021) 14(11):2959. doi: 10.3390/ma14112959.
[32] J. P. Hamilton, C. G. Pantano, Effects of glass structure on the corrosion behavior of sodium-aluminosilicate glasses, J. Non-Cryst. Solids 222 (1997) 167-174.

[33] E. Le Bourhis, Glass: Mechanics and Technology: Second Edition, 2014. Wiley-VCH Verlag GmbH & Co. KGaA, Boschstr. 12, 69469 Weinheim, Germany. ISBN:9783527337057. https://doi.org/10.1002/9783527679461
[34] P. Sundberg, L. Grund Bäck, R. Orman, J. Booth, S. Karlsson, Simultaneous chemical vapor deposition and thermal straightening of glass, Thin Solid Films 669 (2019) 487-493. 10.1016/j.tsf.2018.11.028
[35] N. Sheth, A. Howzen, A. Campbell, H. Liu, C. Pantano, S. Kim, Effects of tempering and heat strengthening on hardness, indentation, fracture resistance and wear of soda lime float glass, Int. J. Appl. Glass Sci.10 (2019) 431-440. 10.1111/ijag.13507
[36] S. Fearn, D.S. McPhail, V. Oakley, Moisture attack on museum glass measured by SIMS, Phys. Chem. Glass 46 (2005) 505–511.
[37] R. Hellmann, S. Cotte, E. Cadel, S. Malladi, L.S. Karlsson, S. Lozano-Perez, M. Cabié, A. Seyeux, Nanometre-scale evidence for interfacial dissolution-reprecipitation control of silicate glass corrosion, Nature Mater. 14 (2015) 307–311. https://doi.org/10.1038/nmat4172
[38] K. Cummings, W.A. Lanford, M. Feldmann, Weathering of glass in moist and polluted air, Nucl. Instrum. Methods Phys. Res. B 136–138 (1998) 858–862. https://doi.org/10.1016/S0168-583X(97)00758-1